

Long-Term Dynamics of Forest Fires in Southern Siberia

E. G. Shvetsov^{a, b, *}, A. S. Golyukov^{b, c, d}, and V. I. Kharuk^{b, c, d}

^a *Khakassian State University, Abakan, 655017 Russia*

^b *Sukachev Institute of Forest of the Siberian Branch of the Russian Academy of Sciences, Separate Subdivision of the FRC KSC SB RAS, Krasnoyarsk, 660036 Russia*

^c *Siberian Federal University, Krasnoyarsk, 660041 Russia*

^d *Tomsk State University, Tomsk, 634050 Russia*

*e-mail: eugeneshvetsov11@yandex.ru

Received December 9, 2022; revised December 18, 2022; accepted December 28, 2022

Abstract—The research focus. Wildfire is a critical environmental disturbance affecting forest dynamics, succession, and the carbon cycle in Siberian forests. Forests of southern Siberia experienced an increase of fire rate. We analyzed spatial and temporal dynamics of burned area in the southern Central Siberian Mountains. We considered burning rate within different forest types: dark needle conifers (DNC) composed by Siberian pine, spruce and fir, light-needle composed by Scotch pine and larch, and mix wood (composed by birch, aspen and conifers). **Methods.** We used long-term (1982–2021) climatic variables from the ERA5-Land database. Satellite observations included MODIS wildfire data (2002–2021) and gravimetric (GRACE) data (2002–2021) for estimation soil moisture content. We analyzed the spatial distribution of burned areas considering dominant forest stands and terrain (elevation, slope aspect and steepness). **Results.** We found a significant decreasing trend in burned area. On average, about 978.7 ± 447.5 thousand ha including 257.1 ± 154.3 thousand ha of forests are disturbed by fire annually. Light coniferous forests are characterized by the highest degree of the fire disturbance (relative burned area, RBA, was ca. 0.83% per year); whereas DNC stands have the lowest RBA (ca. 0.15% per year). The spatial distribution of fires in light coniferous forests showed predominance of fires on the southern slopes comparing to northern slopes (by 15–20%). We found a decreasing logarithmic trend in burned area between plains and low mountains and high mountains due to lower forest fuel loads and increased amount of precipitation on higher elevations. We also observed lower RBA values (by 300–400%) on steep slopes for light coniferous forests and mixed forests comparing to gentle slopes due to lower available forest fuels. The long-term dynamics of burned area in the region was related to the variation of climatic variables, such as soil moisture ($r^2 = 0.70$, $p < 0.01$), moisture content ($r^2 = 0.63$, $p < 0.01$) and drought index ($r^2 = 0.3$, $p < 0.05$).

Keywords: wildfires, Siberian forests, mountain fires, climate-driven burning rate

DOI: 10.1134/S1995425523020154

INTRODUCTION

Wildfire is the most significant factors affecting the boreal forests including vegetation dynamics, biodiversity, and the carbon cycle (*Russian forests...*, 2020). During the last decade, forests of Eurasia and North America experienced a significant increase in the annual burned area (Hanes et al., 2019; Kharuk et al., 2021). For instance, mean annual burned area in Canadian boreal forests is about 1.7 million ha reaching 6 million ha in extreme fire years (Coops et al., 2018). In Russian forests annual burning rate estimated ca. 5–7 million ha with extremes exceeding 10 million ha (Bartalev et al., 2015; Kharuk et al., 2021). In particular, wildfires of 2020 in the western USA were considered as the most destructive wildfires resulted in thousands of smoke-related deaths, buildings that have been damaged or destroyed (Higuera and Abatzoglou, 2020).

Climate change is dominant factors affecting fire frequency and area burned by wildfires in Siberia (Kharuk et al., 2008; Kharuk and Ponomarev, 2017).

Extreme wildfires in Siberia coincided with extremely high temperatures (Kharuk et al., 2021). Current scenarios of climate change predict an increase of air temperatures as well as redistribution of precipitation in Siberia (IPCC, 2014). This will result in a change of fire regime in the region, including fire frequency and intensity, as well as the duration of fire seasons (Shvidenko and Schepaschenko, 2013; Kharuk et al., 2021).

Landscape topography, such as slope and aspect affect the spread of fire and largely determine the spatial distribution of fires (Meigs et al., 2020). For instance, Kharuk et al. (2008) report shorter fire return intervals on southwestern slopes in central Siberia comparing to northeastern slopes. In southern Siberian Mountain fire frequency decreased from plains to highlands (Ponomarev et al., 2016).

Application of remote sensing data enables multiple daily observations of the large areas which makes it possible to assess the degree of fire disturbance and to monitor the post-fire dynamics of forest ecosystems. This is

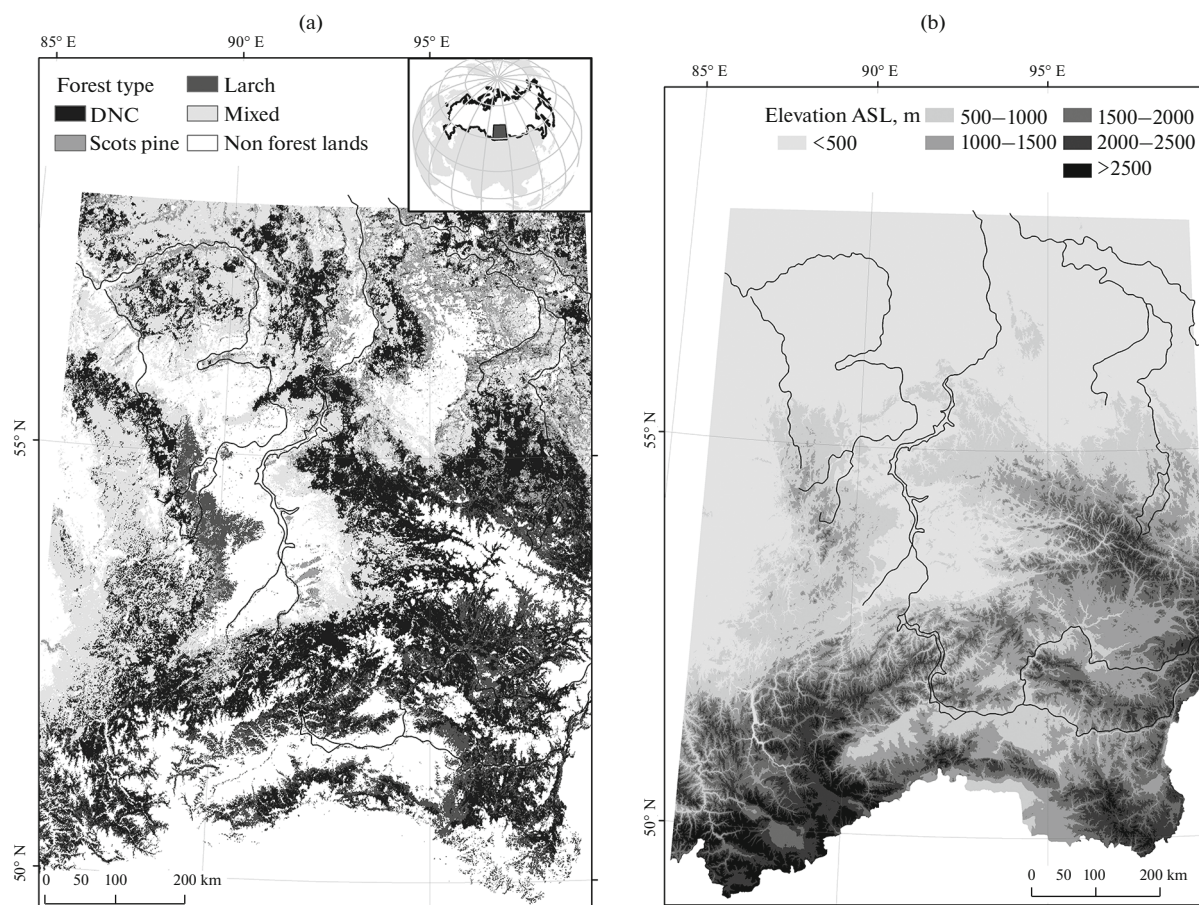


Fig. 1. Study area location. (a) Dominant forests types. DNC are the stands formed by Siberian pine, fir and spruce. (b) Terrain elevations above sea level.

a necessary basis for further research of the state of forest ecosystems in the boreal zone and predicting their stability in a changing climate. Remote sensing is widely used for wildfire detection and burned area estimation (García-Lázaro et al., 2018; Shvetsov et al., 2021). Satellite data also have been widely used to study the process of vegetation recovery after disturbance and to obtain relationships between the fire parameters and the post-fire state of forest ecosystems (Cuevas-Gonzalez et al., 2009; Shvetsov et al., 2019).

Spaceborne soil moisture data obtained by ESA's Soil Moisture and Ocean Salinity (SMOS) and the NASA's Soil Moisture Active Passive (SMAP) missions also provide useful tools in the study of the drought-wildfire relationship (Chaparro et al., 2016). Gravity Recovery and Climate Experiment (GRACE) mission has provided estimates of the Earth's gravitational field which depends, in particular, on water mass. Among other applications GRACE data have also been used to predict wildfire occurrence (Jensen et al., 2018).

In this paper, we used long-term (1982–2021) climate data and satellite fire data (2002–2021) to assess the spatial and temporal dynamics of burned area as

well as its relationship with eco-climate variables. We applied also satellite gravimetric (GRACE) data for estimation of on-ground moisture content and its relevance to the burning rate.

The aim of this study is an analysis of long-term burning rate dynamics in the south of Central Siberia. The tested hypothesis is: fire rate dependent on topo features, forest types, and on-ground moisture content.

The questions to answer:

- (1) What is the seasonal and annual dynamics of burned area?
- (2) How burned area depends on terrain topo features (elevation, slope aspect and steepness)?
- (3) How burned area depends on the eco-climate variables?

DATA AND METHODS

Study Region

The study area is located in the southern regions of central Siberia (50°–58° N and 86°–99° E) and occupies about 7.5×10^5 km² (Fig. 1). Forests occupy about 64% of the study area according to land cover map

developed in Space Research Institute of Russian Academy of Sciences (Bartalev et al., 2016; <http://pro-vega.ru/maps/>). The dominant tree species include larch (*Larix sibirica*) (19% of the forest area), Siberian pine (*Pinus sibirica*) (16%), fir (*Abies sibirica*) (14%), pine (*Pinus sylvestris*) (13%). A significant part of the forest area in the region (33%) is covered by mixed forests with a predominance of deciduous species (*Betula spp.*, *Populus tremula*).

The study region includes several natural zones characterized by different climatic and forest conditions, such as taiga, forest-steppe and southern Siberian mountain zone. The northern part of the region is dominated by plains and lowlands with elevations ranging from 100 to 650 m. Prevailing forest types include pine-dominant and mixed stands (Fig. 1). Southern part of the region includes East and West Sayan Mountains and is characterized by higher elevations ranging between 500 and 3400 m above sea level. Forest stands in the southern part are represented mainly by dark needle coniferous (DNC, i.e., formed by *Pinus sibirica*, *Abies sibirica* and *Picea obovata*) and light coniferous (LC, i.e., formed by *Larix sibirica* and *Pinus sylvestris*) mountain taiga. DNC stands are composed by Siberian pine, spruce and fir dominant forests, whereas LC stands are represented by larch and pine forests. According to ASTER GDEM product lowlands with elevations up to 500 m occupy about 43% of the study area and mountain regions with elevations 1500 m and higher occupy 21% of the region.

Datasets and Methods

For burned area estimation we used long-term series of remote sensing data obtained from several sources. First, as a primary data source we used the wildfire database of the V.N. Sukachev Institute of Forest, generated from TERRA/AQUA MODIS active fire detections. However, this primary database contained data gaps for several years which were filled using the thermal anomaly products from MODIS (MOD14/MYD14 collection 6). MODIS data were downloaded using the LAADS (Level-1 Atmosphere Archive & Distribution System) service (<https://ladsweb.modaps.eosdis.nasa.gov/>). General burned-area mapping approach was based on aggregation of active fire hotspots obtained from the MODIS data products. A similar approach was used in several previous studies (Shvetsov et al., 2021). We also implemented a correction procedure to account for the low resolution of MODIS fire data (Shvetsov et al., 2021). The resulting fire data were stored as vector polygonal layers suitable for further processing using GIS.

We used data from the Vega-service developed in the Space Research Institute Russian Academy of Science (<http://pro-vega.ru/maps/>) (Bartalev et al., 2016) to determine prevailing forest types. This land cover dataset was used to determine the fractions of burned area for each dominant forest type.

Terrain datasets, such as elevation, aspect and slope were obtained using ASTER global digital elevation model of version 3 (Abrams et al., 2020). This dataset was downloaded from the NASA Earthdata service (<https://earthdata.nasa.gov/>) and provides terrain elevation data with spatial resolution of about 30 m. Slope and aspect raster layers were created using GIS software.

For our study area we defined 13 elevation classes with equal step of 250 m, i.e. 0–250, 250–500 m, etc. The final class included all areas with elevation above 3000 m. Slopes were also divided into several classes with the step of 5° (0°–5°, 5°–10°, etc.). The separate class contained all slopes greater than 40°. All slopes larger than 5° were further classified according to their aspect into 8 classes: north, northeast, east, southeast, south, southwest, west and northwest.

Using GIS software we calculated intersections between land cover (dominant tree species), topography (elevation, aspect, slope) and burned area polygons. For each land cover/topography class we calculated mean annual relative burned area as $RBA = 100\% S_{\text{burned}}/S_{\text{class}}$, where S_{burned} is mean annual burned area within the given class (ha) and S_{class} is the area of this class (ha).

Monthly air temperature (°C), precipitation (mm) and soil moisture (SM) data (m^3/m^3 ; covered soil depth ca. 28 cm) obtained from the ERA5-Land database (<https://cds.climate.copernicus.eu/cdsapp#!/dataset>; grid cell size $0.1^\circ \times 0.1^\circ$; period 1950–2020) (Hersbach et al., 2018). Monthly data on moisture content at the entire depth of content in the soil are obtained from GRACE/GRACE-FO satellite data as equivalent water thickness anomalies (EWTA) from the product of the processing level L3 of the GFZ data center (cm, spatial resolution $1^\circ \times 1^\circ$; period 2002–2020) (Landerer et al., 2020). Two satellites fly in orbit one after the other, constantly measuring the distance between them. As soon as the first satellite flies over an object with a large mass, its angular velocity increases, as does the distance to the other satellite, which is immediately fixed by the second one. The standard products of the GRACE project are sets of spherical harmonic coefficients describing the monthly changes in the Earth's gravitational field. By processing level L3, these values can be interpreted as changes in the water mass.

Monthly drought index SPEI (Standardized Precipitation Evapotranspiration Index) dataset was downloaded using SPEI Global Drought Monitor (<http://sac.csic.es/spei/map/maps.html>). SPEI drought index represents the difference between precipitation (P) and potential evapotranspiration (PET) and is calculated as $SPEI = P - PET$ (Vicente-Serrano et al., 2010). Spatial resolution for SPEI dataset was also $1^\circ \times 1^\circ$.

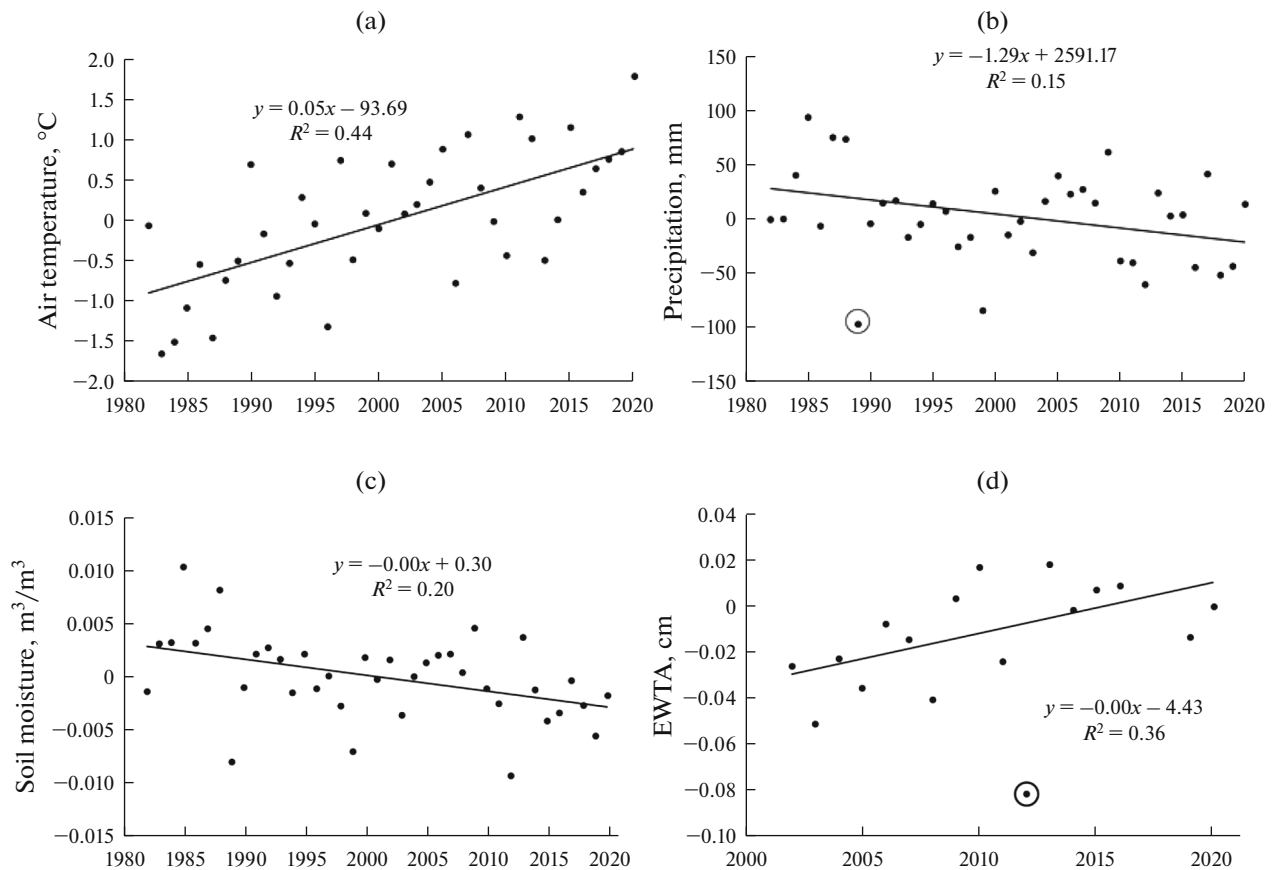


Fig. 2. Dynamics of eco-climate variables in the region: (a) mean summer air temperature anomalies; (b) summer precipitation amount; (c) summer soil moisture; (d) summer EWTA (equivalent of soil moisture anomalies, or terrestrial water storage). Outliers (circled) were excluded from the analysis.

Statistical Analysis

Using Shapiro Wilk test we have found that statistical distribution of annual burned areas could not be considered as normal. Since that we used the non-parametric Spearman test method to analyze annual burned areas. To measure the significance of statistical relationships we considered two levels of significance ($p = 0.01$ and $p = 0.05$).

To check if difference in burned area is significant between the first and the second half of our study period we used Wilcoxon rank sum test.

RESULTS

Temporal Dynamics of Eco-Climatic Variables

An analysis of time series of climatic and soil moisture data showed an increase in summer air temperatures and decrease in precipitation amount (Figs. 2a, 2b). An increase in summer air temperature in the region was found to be statistically significant ($r^2 = 0.44$, $p < 0.01$) with the rate of $0.05^\circ\text{C}/\text{year}$. Long-term decreasing trend in precipitation amount was not significant ($r^2 = 0.15$, $p = 0.08$). We have also

observed a significant decreasing trend ($r^2 = 0.20$, $p < 0.05$) in soil moisture content (Fig. 2c). However, since 2002 (since GRACE gravimetric data became available) the terrestrial water storage (EWTA) was increasing ($r^2 = 0.36$, $p < 0.05$) (Fig. 2d). The possible reason for the increase of terrestrial water storage could be a permafrost thaw of glaciers in the mountains.

Burned Area Dynamics in the Region

Annual burned areas in the region were highly variable depending on weather conditions. Mean annual burned area between 2002 and 2021 was 978.7 ± 447.5 thousand ha (mean \pm SD); non-forest burned area was 721.6 ± 304.5 thousand ha and forest burned area— 257.1 ± 154.3 thousand ha. The largest annual burned area was observed in 2003 (1.6 million ha), and the smallest in 2013 (172.7 thousand ha). The largest forest burned area (537 thousand ha) was also observed in 2003, and the smallest (31.1 thousand ha) in 2021.

The dynamics of burned area within the study region is shown in Fig. 3. Between 2002 and 2021 we found a decrease in the annual burned area in the

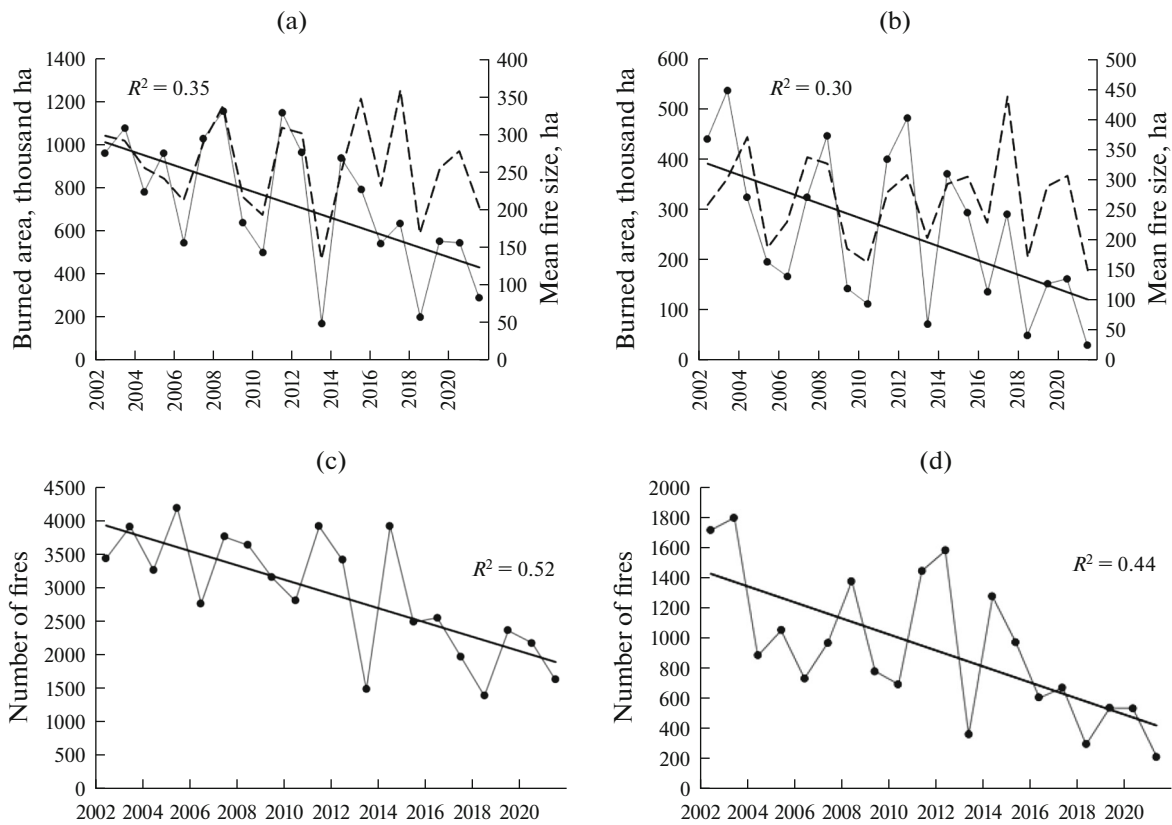


Fig. 3. Burned area (solid line) and mean fire size (dashed line) dynamics on (a) non-forest lands; (b) forest lands. Lower panels show the number of fire events on (c) non-forest and (d) forest lands.

region. The linear regression was statistically significant for fires on forest ($r^2 = 0.3$; $p < 0.05$) (decrease rate—14 thousand ha per year) and non-forest lands ($r^2 = 0.35$; $p < 0.01$) (decrease rate – 30 thousand ha per year). We also found a statistically significant relationship between annual burned area and mean fire size on both forest ($r^2 = 0.4$; $p < 0.01$) and non-forest ($r^2 = 0.54$; $p < 0.01$) lands (Fig. 3). This means that during large fire years fires tend to have larger mean size. At the same time we have not found significant interannual trend in mean fire size ($r^2 = 0.01$; $p = 0.6$). Temporal dynamics of the number of fire events also showed a significant decreasing trend on both non-forest ($r^2 = 0.52$; $p < 0.01$) and forest lands ($r^2 = 0.44$; $p < 0.01$) (Fig. 3). Additionally, we have compared the differences in mean annual burned area between two decades (2002–2011 and 2012–2021). Mean annual burned area between 2002 and 2011 was 879.7 ± 245.8 thousand ha and decreased to 563.4 ± 282.4 thousand ha in 2012–2021. Wilcoxon rank sum test showed a significant difference in burned area between these two periods ($p < 0.05$).

Fires on non-forest lands accounted for about $75.3 \pm 6.2\%$ of the burned area (Fig. 4) with the RBA of 3.2%. Most of the area burned by forest fires

occurred in the mixed forest stands ($12.2 \pm 5.6\%$). At the same time, the mean annual value of the relative burned area for this forest type was 0.67%. Larch-dominant forests accounted for $7.9 \pm 4.2\%$ of the annual burned area with the RBA of 0.81%. Mean

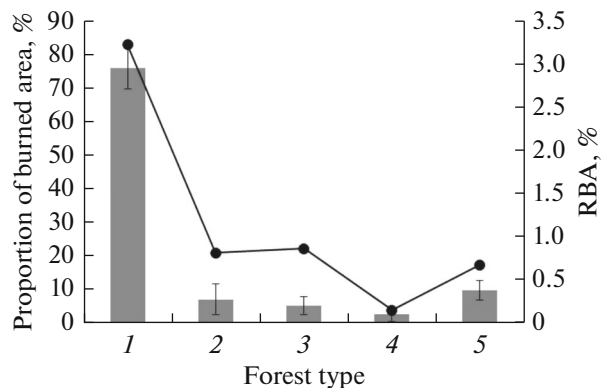


Fig. 4. Proportion of burned area and RBA (relative burned area) in the different forest types. (1) Non-forest lands; (2, 3, 4) larch-dominant, pine-dominant and DNC stands, correspondingly; (5) mixed forests. Bars indicate proportion of burned area; error bars corresponded to one standard deviation. RBA is shown by solid line.

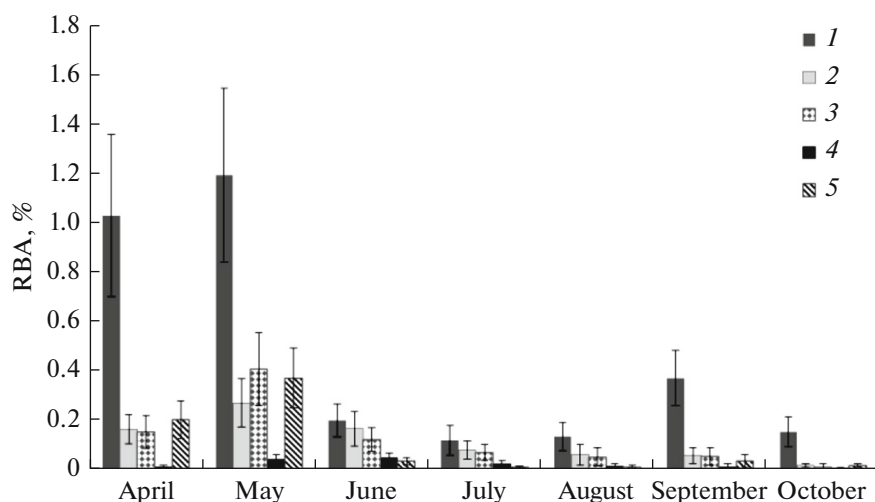


Fig. 5. Seasonal distribution of the RBA (relative burned area). Land cover types: (1) non forest lands; (2) larch-dominant, (3) pine-dominant, (4) DNC-dominant and (5) mixed forests. Error bars correspond to one standard deviation. The highest RBA values which observed in April–May accounting for about 65% of the total burned area.

annual burned areas in pine and dark needle coniferous stands were estimated as $6.4 \pm 4.4\%$ and $4.7 \pm 3.8\%$, respectively. Corresponding RBA values for these forest types were 0.86 and 0.15%, respectively (Fig. 4).

Temporal distribution of burned areas during the fire season has a well-defined maximum, which occurs in the second half of spring. April and May account for about 65% of the total area burned by wildfires during the fire season (Fig. 5) with relative burned area exceeding 1%. Analysis of the seasonal dynamics of fires considering individual forest types shows that in mixed forest stands, as well as in larch and pine dominant stands, the largest burned areas were detected during May. At the same time, in forest stands with a predominance of dark needle coniferous species, significant burned areas were also observed during the summer months (June, July) (Fig. 5). Forest lands were characterized by significantly lower RBA values reaching 0.4% for pine-dominant and mixed stands. The lowest RBA was observed for DNC stands reaching 0.05% in June. It also should be noted that monthly burned areas are characterized by significant variability (high values of the standard deviation) depending on weather conditions.

Burned Area vs Eco-Climate Variables

Analysis of the relationships between burned area in the region and several climatic and geophysical variables showed significant correlation ($r^2 = 0.30$, $p < 0.05$) between burned areas and drought index SPEI during fire season (April–October) (Fig. 6a). We have found a strong influence of the soil moisture on burned area ($r^2 = 0.70$, $p < 0.01$) in May, when most of the burning in the region occurs (Fig. 6b). However,

the terrestrial water storage (EWTA) measured during summer months (July, August) was found to be related better with burned area ($r^2 = 0.63$, $p < 0.01$) (Fig. 6c). Finally, the precipitation amount, similarly to soil moisture, shows the highest correlation with burned area in May ($r^2 = 0.4$, $p < 0.01$) (Fig. 6d). At the same time, we have not found any significant relationship between air temperature and burned area ($r^2 = 0.01$, $p = 0.65$).

Terrain Effects on Burned Area Distribution

According to the terrain analysis the highest RBA values (2.5–3.6%) was observed in larch-dominated forests growing at elevations up to 500 meters above sea level (Fig 7), i.e. up to 3.6% of the larch forests area below 500 m is damaged by fires every year. At the same time, RBA decreased with the increase of the elevation for all forest types except dark-coniferous stands (Fig. 7). Thus, at elevations of 1500 meters above sea level and higher, the RBA value for all dominant types of forest stands did not exceed 0.8%. In case of dark needle coniferous forests, RBA does not change significantly with elevation and amounts to 0.1–0.3%. The change of RBA with elevation was fitted using a logarithmic function: $RBA = A \cdot \log(\text{Elevation}) + B$. Coefficient A varied from -1.3 for larch forests ($r^2 = 0.79$) to -0.02 for dark needle coniferous forests ($r^2 = 0.01$).

Analysis of burned area distribution (Fig. 8a) has not showed a significant predominance of burned area on any aspect. Larch and pine dominant stands as well as mixed forests generally had somewhat higher RBA values on southern slopes (Fig. 8a). For instance, mean RBA value for larch-dominated forests was 0.95% on southern slopes and 0.82% on northern

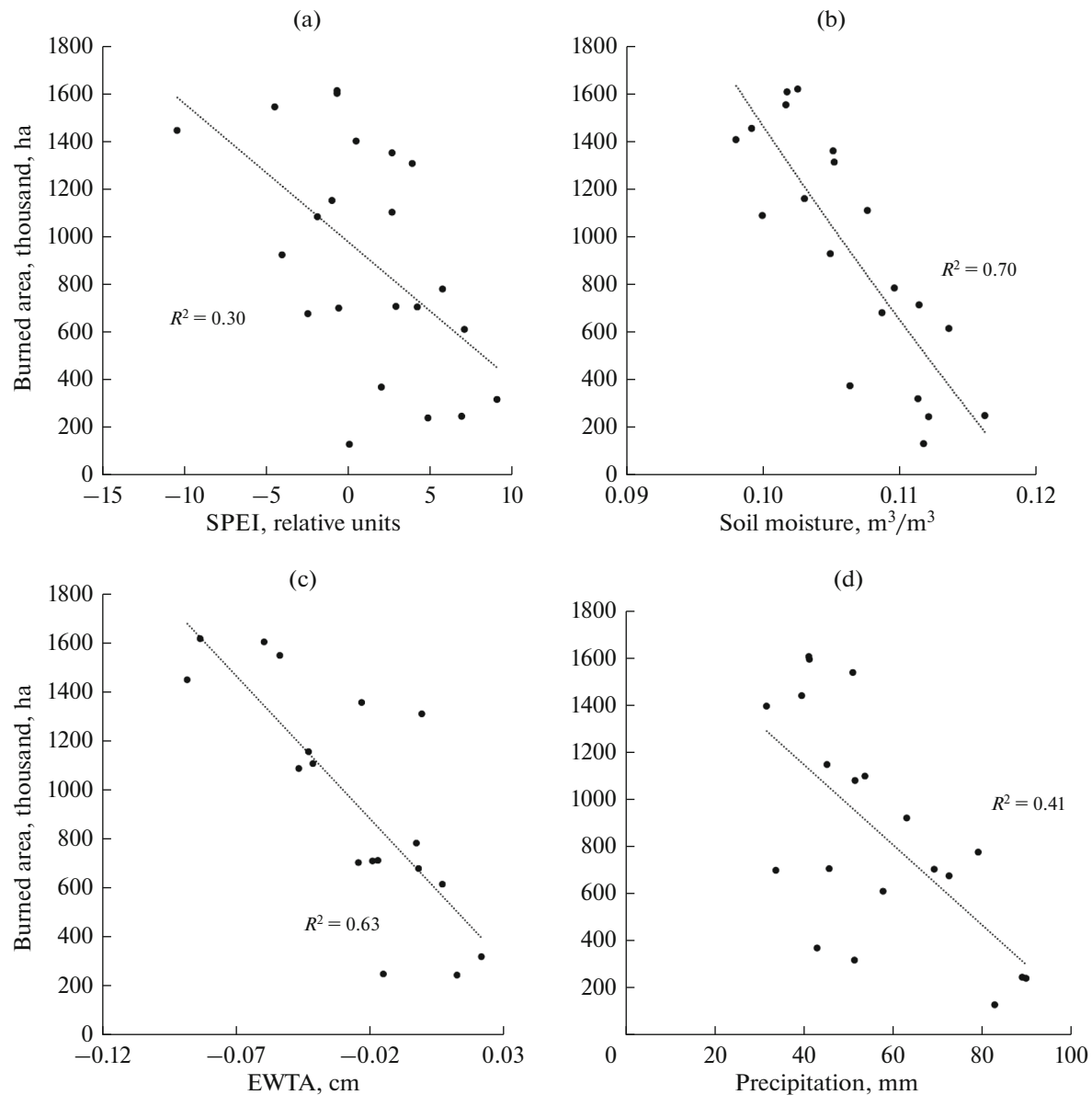


Fig. 6. Relationships between burned area several climatic and geophysical variables. Mean drought index SPEI and burned area for the whole fire season (Apr–Oct) (a); Monthly (May) soil moisture and burned area (b); Mean summer (July–August) EWTA and burned area (c); Precipitation amount for May and burned area (d).

slopes. For pine-dominant stands these values were 1.08 and 0.80%, respectively. At the same time in case of dark needle coniferous stands eastern and eastern and north-eastern slopes were found to have slightly higher RBA values (0.19%) comparing to other aspects (0.17% on average).

Figure 8b shows the distribution of RBA values according to slope steepness. For all prevailing forest types RBA decreased with the increase of slope. The highest RBA values (1.0–1.5%) were calculated for larch-dominant forests on gentle slopes (below 10 degrees). For pine-dominant stands and mixed forests RBA values on gentle slopes were lower com-

paring to larch forests—1.1 and 0.8%, respectively. The lowest RBA values as well as the lowest rate of change were found for the dark needle coniferous stands (0.1–0.2% for all classes of slopes).

With the increase of slope a decrease in RBA was observed, which was fitted using a logarithmic function: $RBA = A \cdot \log(\text{Slope}) + B$. In the case of slope, coefficient A varied from -0.58 for larch forests ($r^2 = 0.98$) to -0.04 for DNC forests ($r^2 = 0.50$).

At elevations below 750 m mixed forests prevail, however elevation range between 750 and 2000 m above sea level is covered mainly by larch and dark needle

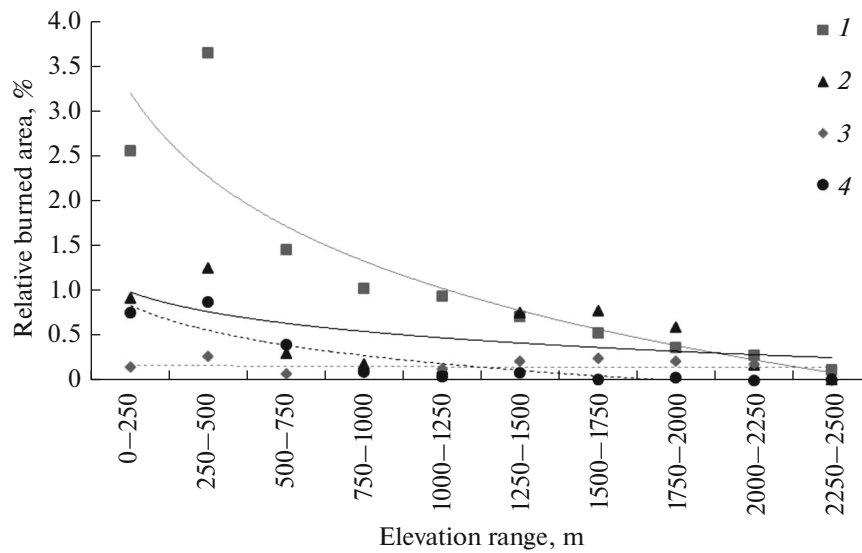


Fig. 7. Relative burned area (RBA) dependence on forest types and elevation. Forest types: (1, 2) larch-dominant and pine-dominant forests; (3, 4) DNC and mixed forests. Solid lines indicate logarithmic trends. RBA for all dominant forest type except DNC forests decreased with elevation.

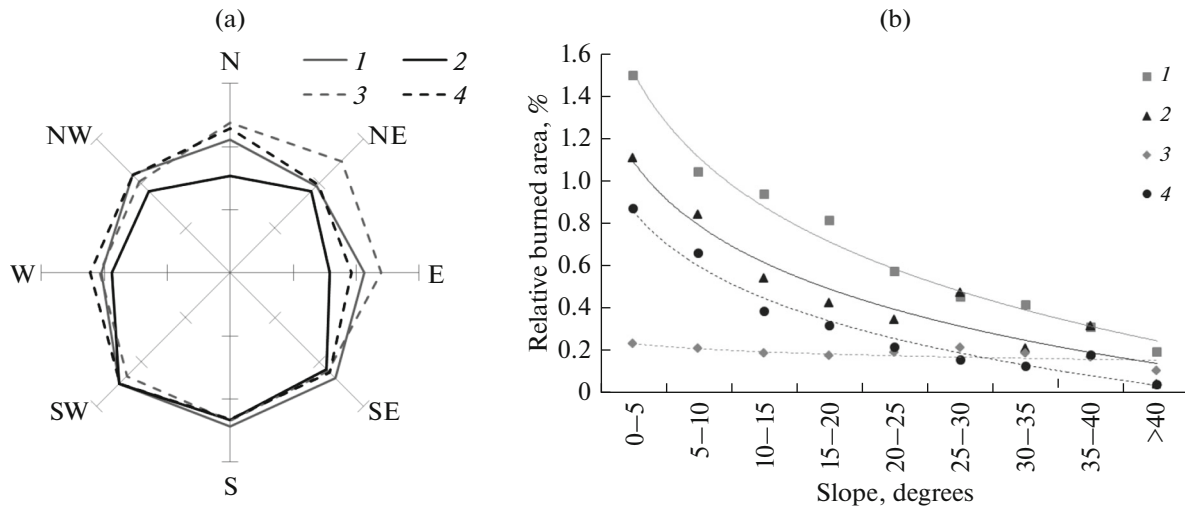


Fig. 8. Relative burned area dependence on (a) aspect and (b) slope steepness. Solid lines indicated logarithmic trends. Forest types: (1) larch-dominant forests; (2) pine-dominant forests; (3) DNC forests; (4) mixed forests. Larch and pine dominant stands have somewhat higher RBA values on southern slopes whereas DNC forests on eastern and north-eastern slopes are characterized by slightly higher RBA values. Relative burned area for all dominant forest type except DNC forests decreased with slope steepness decrease.

coniferous stands (Supplementary data, Fig. S1). We found that the forest fraction decreased with the increase of elevation. For instance, only 23% of area located above 2000 m was covered by forests while for the other elevation ranges this proportion varied between 44 and 81%.

The proportion of the area covered by forests varied depending on aspect, ranging from 55% for south-eastern slopes to 63% for northern and north-western

slopes (Supplementary data, Fig. S2). We found a significant decrease of the forest-covered area on steep slopes ($>30^\circ$). Mean proportion of forest covered area was 32% at steep slopes ($>30^\circ$) and it was two times higher (65%) for less steeper slopes (less than 30°). We can also note that pine-dominated and mixed forests were mainly located at elevations below 1000 m and slopes $<15^\circ$. Larch and dark needle coniferous forests prevailed at elevations over 750 m (Supplementary data, Figs. S1, S3).

DISCUSSION

The dynamics of burned area in various regions that is influenced by many factors including climate, ignition sources, and vegetation properties can vary significantly, often having opposite dynamics (Forkel et al., 2019). For example, in Russia between 2001 and 2016 there was a decrease in burned area on non-forest lands. At the same time, an increase in burned area was observed on forest lands, mainly in the larch forests of Central and Eastern Siberia (Loupian et al., 2017). It can be noted that opposite burned area trends are observed for different regions of Siberia. The increasing trend in the number of fires and burned area over the past decades was also found for various larch-dominant regions of Siberia (Kharuk and Ponomarev, 2017; García-Lázaro et al., 2018; Kharuk et al., 2021). However, in the pine-dominant forests of Angara region in Central Siberia regression analysis did not show any significant trend in burned area between 2002 and 2020 (Shvetsov et al., 2021) and in the southern regions of western Siberia, there was a decline in burned area (Tomshin and Soloviev, 2021). Within our study region we have found a burned area decline since 2002 mostly caused by the last four years (2018–2021) with low burned areas. For our study area, we have not found significant changes in the mean fire area. At the same time, in other regions, for example, in the western U.S. an increase in the mean fire area was observed (Dennison et al., 2014).

The majority of fires were detected on non-forest lands and in mixed forests (Fig. 4). The results of geospatial analysis showed that of the fires in mixed forests were located mostly within the boundary with non-forest lands. Similar observations, i.e. propagation of non-forest fires to the adjacent forest lands also reported by Kukavskaya et al. (2016) and Shvetsov et al. (2021). Notably that seasonal distribution of fires in mixed forests correlates well with the distribution of fires on non-forest lands (Fig. 5).

Climate is one of the most important factors controlling the wildfire dynamics. As it was shown previously, the number of fires in Siberia is related with summer temperature anomalies (Kharuk and Ponomarev, 2017). However, we have not found significant correlations between burned area dynamics and air temperature within the study region. Standardized Precipitation Evapotranspiration Index (SPEI) was previously shown to have moderate correlation with burned area in the northern regions of Siberia (Kharuk et al., 2022). Considering the study region SPEI drought index have shown the similar moderate correlation with burned area.

Previous study by Korovin (1996) showed that southern regions of Russia generally experience bimodal distribution of number of fires with main peak occurring in late April and May and lower secondary peak in September and early October. In our study we found that fires on non-forest lands and in mixed for-

ests follow this pattern with two peaks of burned area occurring in late spring and early autumn. At the same time seasonal distribution of burned area for other forest types was unimodal (Fig. 5) with most of the fires detected during spring (April and May), which is typical for the Southern Siberia (Kukavskaya et al., 2016). In herbaceous types of forests in spring low humidity in combination with winds facilitated ground cover dry out, and, by that, promoted fires spread over large areas. In summer, a significant decrease in burned area occurred due to the appearance of green grasses and shrubs. Meanwhile in the DNC, where grass cover poor in comparison with mix woods, a significant fraction (about 45%) of burned area occurred during summer (June and July). The DNC forests are characterized by low to moderate level of fire danger. It also should be noted that while spring fires in Siberia are usually low to moderate-severity surface fires, summer fires which occurred during dry weather (e.g., during Siberian anticyclone period) have higher severity which often result in high tree mortality (Kharuk et al., 2021).

Fire occurrence and burned area distribution in the mountain forests is determined by many factors, including slope steepness and aspect, the shape and size of intermountain basins, vegetation types and local winds (mountain-valley wind circulation) (Flatley et al., 2011). Topographic features, such as slope and aspect can influence fire spread rate and fireline intensity as well as spatial distribution of burn patches across the landscape (Beaty and Taylor, 2001; Alexander et al., 2006). At the same time, elevation influences fuel type and fuel moisture affecting the conditions for fire ignition (Swetnam et al., 2011). The influence of topographic factors on the occurrence of fires and their characteristics varies between different regions. For instance slope and elevation were significant predictive variables for fire ignition occurrence and frequency in Southern California (Faivre et al., 2014). At the same time slope and aspect were not considered as important factors for determining fire occurrence in northeastern China (Wu et al., 2014). For our study region we found a decreasing logarithmic trend in burned area between plains and low mountains and high mountains. The possible reason for that could be a decrease of fuel load and increased amount of precipitation on higher elevations. The highest values of relative burned area in all forest types were observed for plains with elevations below 500 m and within intermountain basins (Fig. 7). A significant number of fires that occur in such areas was also reported for the Altai-Sayan region (Ponomarev et al., 2016). Considering the burned area distribution by slope aspect we found that somewhat higher (15–20%) RBA values were observed on southern slopes (southern, southeastern and southwestern slopes). We also found a decrease of RBA with slope steepness increase for all dominant tree stands except for DNC forests. Light coniferous and mixed forests growing on gentle slopes ($<10^\circ$) were characterized by 300–400% higher

RBA values comparing to steep slopes ($>30^\circ$). This probably could be explained by reduction of available forest fuels on steeper slopes (Supplementary data, Fig. S3).

CONCLUSIONS

We found a significant trend of burned area decrease in the southern regions of Central Siberia since 2002. Mean burned area between 2012 and 2021 was 34% lower comparing to 2002–2011. However, we have not found significant change in mean fire size between 2002 and 2021. Burned area in the region was strongly correlated with soil moisture anomalies (GRACE-derived and ERA-5 modeled data) ($r^2 = 0.63–0.70$). Correlations between burned area and atmospheric (or ambient air) drought measured by drought index (SPEI) anomalies were also observed ($r^2 = 0.30$).

Relative burned area of non-forest (forest-steppe) zone was almost four times higher comparing to forest zone. The highest RBA value within forest zone was observed in larch and pine-dominant forests (0.81–0.86%) followed by mixed forests (0.67%). DNC stands were characterized by the lowest RBA of 0.15%. The analysis of the seasonal dynamics of burned area in the region showed apparent bi-modal distribution for non-forest zone and to a lesser extent for mixed forests. At the same time for larch and pine dominant stands a unimodal distribution with the pronounced maximum occurring in May was observed when RBA reached 0.27 and 0.41% for larch and pine dominant stands respectively. At the same time for DNC forests the highest RBA value (0.05%) was observed in June.

Lesser fuel load and increased amount of precipitation on higher elevations resulted in logarithmic decrease in burned area between plains and low mountains and high mountains. The highest RBA was observed in forest-steppe (below 500 m a.s.l.) and within intermountain hollows for all dominant tree stands except DNC forests which are characterized by low level of fire danger. In light coniferous forests relative burned area was 15–20% higher on the southern slopes comparing to northern slopes. However, in dark needle coniferous stands on eastern and north-eastern RBA was somewhat (10%) higher.

FUNDING

The study was supported by the Russian Science Foundation and the Government of Republic of Khakassia (grant no. 22-17-20012, <https://rscf.ru/en/project/22-17-20012/>).

CONFLICT OF INTEREST

The authors declare that they have no conflicts of interest.

SUPPLEMENTARY INFORMATION

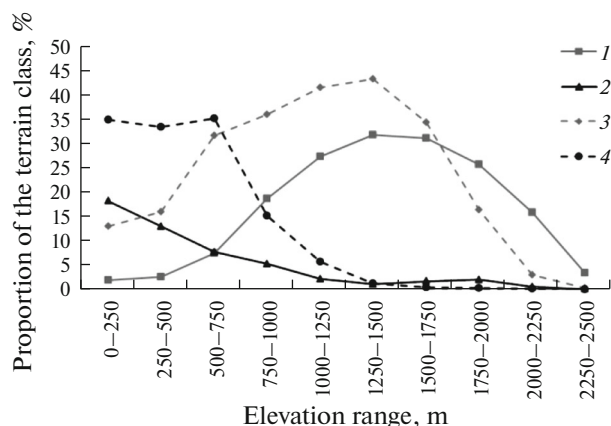


Fig. S1. Forest types distribution along the elevation gradient: (1) larch-dominant stands; (2) pine-dominant stands; (3) DNC stands and (4) mixed forests.

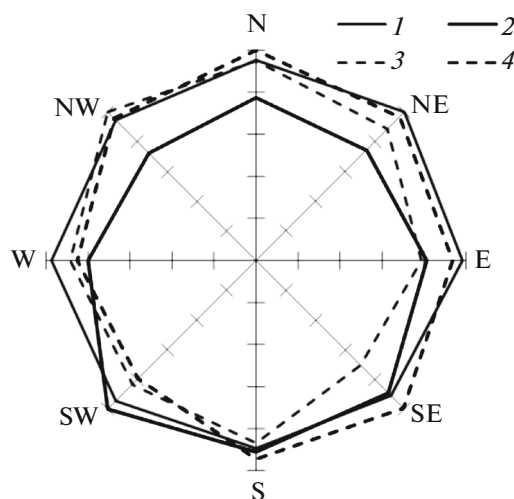


Fig. S2. Forest types distribution for eight aspect classes: (1) larch-dominant stands; (2) pine-dominant stands; (3) DNC stands and (4) mixed forests. Slopes smaller than 5° were not considered for aspect distribution calculation.

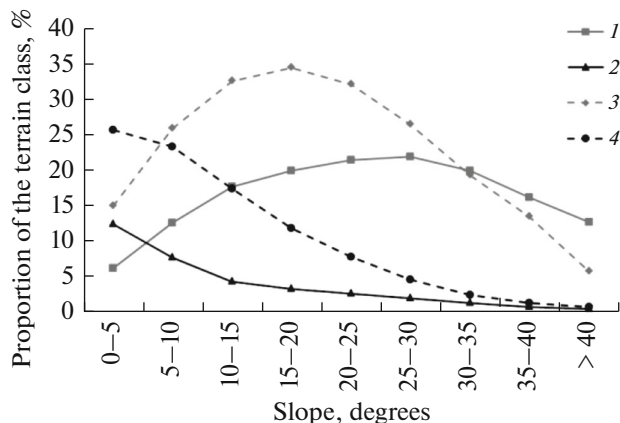


Fig. S3. Forest types distribution along the slope gradient: (1) larch-dominant stands; (2) pine-dominant stands; (3) DNC stands and (4) mixed forests.

OPEN ACCESS

This article is licensed under a Creative Commons Attribution 4.0 International License, which permits use, sharing, adaptation, distribution and reproduction in any medium or format, as long as you give appropriate credit to the original author(s) and the source, provide a link to the Creative Commons license, and indicate if changes were made. The images or other third party material in this article are included in the article's Creative Commons license, unless indicated otherwise in a credit line to the material. If material is not included in the article's Creative Commons license and your intended use is not permitted by statutory regulation or exceeds the permitted use, you will need to obtain permission directly from the copyright holder. To view a copy of this license, visit <http://creativecommons.org/licenses/by/4.0/>.

REFERENCES

- Abrams, M., Crippen, R., and Fujisada, H., ASTER Global Digital Elevation Model (GDEM) and ASTER Global Water Body Dataset (ASTWBD), *Remote Sens.*, 2020, vol. 12, no. 7, p. 1156.
<https://doi.org/10.3390/rs12071156>
- Alexander, J.D., Seavy, N.E., Ralph, C.J., and Hogo-boom, B., Vegetation and topographical correlates of fire severity from two fires in the Klamath–Siskiyou region of Oregon and California, *International Int. J. Wildland Fire*, 2006, vol. 15, pp. 237–245.
<https://doi.org/10.1071/WF05053>
- Bartalev, S.A., Stytsenko, F.V., Egorov, V.A., and Loupian, E.A., Satellite assessment of fire-caused forest mortality in Russia, *Lesovedenie*, 2015, vol. 2, pp. 83–94.
- Bartalev, S.A., Egorov, V.A., Zharko, V.O., Loupian, E.A., Plotnikov, D.E., Khvostikov, S., Shabanov, N., *Sputnikovoe kartografirovaniye rastitel'nogo pokrova Rossii* (Land Cover Mapping Over Russia using Earth Observation Data), Moscow: Inst. Kosm. Issled. Ross. Akad. Nauk, 2016.
- Beaty, R.M. and Taylor, A.H., Spatial and temporal variation of fire regimes in a mixed conifer forest landscape, Southern Cascades, California, USA, *J. Biogeogr.*, 2001, vol. 28, pp. 955–966.
<https://doi.org/10.1046/J.1365-2699.2001.00591.X>
- Chaparro, D., Piles, M., and Vallossera, M., Remotely sensed soil moisture as a key variable in wildfires prevention services: towards new prediction tools using SMOS and SMAP data, in *Satellite Soil Moisture Retrieval*, Srivastava P.K., et al., Eds., Elsevier, 2016, pp. 249–269.
<https://doi.org/10.1016/B978-0-12-803388-3.00013-9>
- Coops, N.C., Hermosilla, T., Wulder, M.A., White, J.C., and Bolton, D.K., A thirty year, fine-scale, characterization of area burned in Canadian forests shows evidence of regionally increasing trends in the last decade, *PLoS One*, 2018, vol. 13, no. 5, p. e0197218.
<https://doi.org/10.1371/journal.pone.0197218>
- Cuevas-Gonzalez, M., Gerard, F., Balzter, H., and Riano, D., Analysing forest recovery after wildfire disturbance in boreal Siberia using remotely sensed vegetation indices, *Global Change Biol.*, 2009, vol. 15, pp. 561–577.
<https://doi.org/10.1111/j.1365-2486.2008.01784.x>
- Dennison, P.E., Brewer, S.C., Arnold, J.D., and Moritz, M.A., Large wildfire trends in the western United States, 1984–2011, *Geophys. Res. Lett.*, 2014, vol. 41, pp. 2928–2933.
<https://doi.org/10.1002/2014GL059576>
- Faivre, N., Jin, Y., Goulden, M.L., and Randerson, J.T., Controls on the spatial pattern of wildfire ignitions in Southern California, *Int. J. Wildland Fire*, 2014, vol. 23, no. 6, pp. 799–811.
<https://doi.org/10.1071/WF13136>
- Flatley, W.T., Lafon, C.W., and Grissino-Mayer, H.D., Climatic and topographic controls on patterns of fire in the southern and central Appalachian Mountains, USA, *Landscape Ecol.*, 2011, vol. 26, no. 2, pp. 195–209.
<https://doi.org/10.1007/s10980-010-9553-3>
- Forkel, M., Dorigo, W., Lasslop, G., Chuvieco, E., Harrison, S., Heil, A., Teubner, I., Thonicke, K., and Harrison, S.P., Recent global and regional trends in burned area and their compensating environmental controls, *Environ. Res. Commun.*, 2019, vol. 1, p. 051005.
<https://doi.org/10.1088/2515-7620/ab25d2>
- García-Lázaro, J.R., Moreno-Ruiz, J.A., Riaño, D., and Arbelo, M., Estimation of burned area in the North-eastern Siberian boreal forest from a Long-Term Data Record (LTDR) 1982–2015 time series, *Remote Sens.*, 2018, vol. 10, p. 940.
<https://doi.org/10.3390/rs10060940>
- Hanes, C.C., Wang, X., Jain, P., Parisien, M.A., Little, J.M., and Flannigan, M.D., Fire-regime changes in Canada over the last half century, *Can. J. For. Res.*, 2019, vol. 49, pp. 256–269.
<https://doi.org/10.1139/cjfr-2018-0293>
- Hersbach, H., Rosnay, P., Bell, B., Schepers, D., Simmons, A., Soci, C., Abdalla, S., Alonso-Balmaseda, M., Balsamo, G., Bechtold, P., et al., Operational Global Reanalysis: Progress, Future Directions and Synergies with NWP, ECMWF ERA Report Series, 2018.
<https://www.ecmwf.int/en/elibrary/18765-operational-global-reanalysis-progress-future-directions-and-synergies-nwp>. Cited October 15, 2022.
- Higuera, P.E. and Abatzoglou, J.T., Record-setting climate enabled the extraordinary 2020 fire season in the western United States, *Global Change Biol.*, 2020, vol. 27, no. 1, pp. 1–2.
<https://doi.org/10.1111/gcb.15388>
- IPCC 2014: *Climate Change 2014: Synthesis Report. Contribution of Working Groups I, II and III to the Fifth Assessment Report of the Intergovernmental Panel on Climate Change*, Pachauri, R.K. and Meyer, L.A., Eds., IPCC, Geneva. https://archive.ipcc.ch/pdf/assessment-report/ar5/syr/SYR_AR5_FINAL_full_wcover.pdf. Accessed October, 26, 2022.
- Jensen, D., Reager, J.T., Zajic, B., Rousseau, N., Rodell, M., and Hinkley, E., The sensitivity of US wildfire occurrence to pre-season soil moisture conditions across ecosystems, *Environ. Res. Lett.*, 2018, vol. 13, p. 014021.
<https://doi.org/10.1088/1748-9326/aa9853>
- Kharuk, V.I., Ranson, K.J., and Dvinskaya, M.L., Wildfires dynamic in the larch dominance zone, *Geophys. Res. Lett.*, 2008, vol. 35, p. L01402.
<https://doi.org/10.1029/2007GL032291>

- Kharuk, V.I. and Ponomarev, E.I., Spatiotemporal characteristics of wildfire frequency and relative area burned in larch-dominated forests of Central Siberia, *Russ. J. Ecol.*, 2017, vol. 48, no. 6, pp. 507–512.
- Kharuk, V.I., Ponomarev, E.I., Ivanova, G.A., Dvinskaya, M.L., Coogan, S.C.P., and Flannigan, M.D., Wildfires in the Siberian taiga, *Ambio*, 2021, vol. 50, pp. 1953–1974
<https://doi.org/10.1007/s13280-020-01490-x>
- Korovin, G.N., Analysis of the Distribution of Forest Fires in Russia, in *Fire in Ecosystems of Boreal Eurasia*, Gollammer, J.G. and Furyaev, V.V., Eds., Dordrecht: Springer-Verlag, 2016, vol. 48, pp. 112–128.
https://doi.org/10.1007/978-94-015-8737-2_8
- Kukavskaya, E.A., Buryak, L.V., Shvetsov, E.G., Conard, S.G., and Kalenskaya, O.P., The impact of increasing fire frequency on forest transformations in southern Siberia, *For. Ecol. Manage.*, 2016, vol. 382, pp. 225–235
<https://doi.org/10.1016/j.foreco.2016.10.015>
- Landerer, F.W., Flechtner, F.M., Save, H., Webb, F.H., Bandikova, T., Bertiger, W.I., et al., Extending the global mass change data record: GRACE Follow-On instrument and science data performance, *Geophys. Res. Lett.*, 2020, vol. 47, p. e2020GL088306.
<https://doi.org/10.1029/2020GL088306>
- Loupian, E.A., Bartalev, S.A., Balashov, I.V., Egorov, V.A., Ershov, D.V., Kobets, D.A., Senko, K.S., Stytsenko, F.V., and Sychugovet, I.G., Satellite monitoring of forest fires in the 21st century in the territory of the Russian Federation (facts and figures based on active fires detection), *Sovrem. Probl. Distantionnogo Zondirovaniya Zemli Kosmosa*, 2017, vol. 14, no. 6, pp. 158–175.
- Ponomarev, E.I., Shvetsov, E.G., and Kharuk, V.I., Fires in the Altai-Sayan region: Landscape and ecological confinement, *Izvestiya, Atmos. Oceanic Phys.*, 2016, vol. 52, no. 7, pp. 725–736
- Russian forests and climate change What Science Can Tell Us*, Leskinen, P., Lindner, M., Verkerk, P.J., Nabuurs, G.J., Van Brusselen, J., Kulikova, E., Hasegawa, M., and Lerink, B., Eds., Eur. For. Inst., 2020, vol. 11.
<https://doi.org/10.36333/wsctu11>
- Shvetsov, E.G., Kukavskaya, E.A., Shestakova, T.A., Laflamme, J., and Rogers, B.M., Increasing fire and logging disturbances in Siberian boreal forests: a case study of the Angara region, *Environ. Res. Lett.*, 2021, vol. 16, p. 115007.
<https://doi.org/10.1088/1748-9326/ac2e37>
- Shvidenko, A.Z. and Schepaschenko, D.G., Climate change and wildfires in Russia, *Contemp. Probl. Ecol.*, 2013, vol. 6, pp. 50–61.
<https://doi.org/10.1134/S199542551307010X>
- Swetnam, T., Falk, D., Hessel, A., and Farris, C., Reconstructing landscape pattern of historical fires and fire regimes, in *The Landscape Ecology of Fire*, McKenzie, D., Miller, C., and Falk, D.A., Eds., London: Springer-Verlag, 2011, pp. 165–192.
- Tomshin, O. and Solovyev, V., Spatio-temporal patterns of wildfires in Siberia during 2001–2020, *Geocarto Int.*, 2021.
<https://doi.org/10.1080/10106049.2021.1973581>
- Vicente-Serrano, S.M., Beguería, S., and López-Moreno, J.I., A Multi-scalar drought index sensitive to global warming: The Standardized Precipitation Evapotranspiration Index, *J. Climate*, 2010, vol. 23, pp. 1696–1718.
<https://doi.org/10.1175/2009JCLI2909.1>
- Wu, Z., He, H.S., Yang, J., Liu, Z., and Liang, Y., Relative effects of climatic and local factors on fire occurrence in boreal forest landscapes of northeastern China, *Sci. Total Environ.*, 2014, vol. 493, pp. 472–480.
<https://doi.org/10.1016/j.scitotenv.2014.06.011>